Cell Tissue Res (2006) 324: 403–410
DOI 10.1007/s00441-006-0158-8

REGULAR ARTICLE

Marco Slesina · Elisabeth M. Inman · Ann E. Moore · Joshua I. Goldhaber · Leonard H. Rome · Walter Volknandt

Movement of vault particles visualized by GFP-tagged major vault protein

Received: 30 June 2005 / Accepted: 4 January 2006 / Published online: 28 February 2006

Abstract Vaults are abundant large ribonucleoprotein particles. They frequently colocalize with microtubules and accumulate in filamentous actin-rich lamellipodia. To examine the movement of vaults in living cells, a chimera between the green fluorescent protein and the major vault protein was created. This fusion protein assembled into vault particles as assayed by biochemical fractionation and direct observation of living or fixed cells. By fluorescence recovery after photobleaching, we analyzed the bulk transport of vault particles into neuritic tips of PC12 cells treated with nerve growth factor. Confocal laser scanning microscopy demonstrated co-localization of the major vault protein and microtubules. Video microscopy indicated that, whereas the majority of vault particles were stationary, some individual vault particles moved rapidly, consistent with the action of a microtubule-based or actin-based molecular motor.

This work was supported by the United States Public Health Service, National Institutes of Health (grant GM38097 to L.H.R.) and by the North Atlantic Treaty Organization (grant CRG972834 to W.V.).

M. Slesina · W. Volknandt (✉)
Biocenter, Zoological Institute, J. W. Goethe University,
Marie-Curie-Strasse 9,
60439 Frankfurt, Main, Germany
e-mail: volknandt@zoology.uni-frankfurt.de
Tel.: +49-69-79829603
Fax: +49-69-79829606

E. M. Inman · A. E. Moore · L. H. Rome
Department of Biological Chemistry, UCLA School of Medicine and the Jonsson Comprehensive Cancer Center,
Los Angeles, CA 90095-1737, USA

J. I. Goldhaber
Department of Medicine/Cardiology,
UCLA School of Medicine,
Los Angeles, CA 90095-1737, USA

Present address:
E. M. Inman
Wound Management R&D, Hyland Immuno Division,
Baxter Healthcare Corporation,
Duarte, CA 91010, USA

Keywords Ribonucleoprotein particles · Green fluorescent protein · Major vault protein · Microtubule association · Vault motility · Rat phaeochromocytoma cells

Introduction

Vaults are cytoplasmic ribonucleoprotein particles (RNPs) of unknown function (for reviews, see Kickhoefer et al. 1996; Rome et al. 1991; Mossink et al. 2003; Van Zon et al. 2003a). In both structure and composition, vaults are highly conserved (Kedersha et al. 1990). Vaults measure ~65×40 nm^2 or approximately three times the size of a ribosome, making them the largest RNP known (Kedersha and Rome 1986); they are hollow and capable of opening into two halves with eight-fold symmetry (Kedersha et al. 1991; Kong et al. 1999, 2000). Rat vaults contain three species of protein and an untranslated 141-base polymerase III RNA transcript yielding an overall mass of ~13 MDa per particle (Kedersha and Rome 1986; Kickhoefer et al. 1993; Kickhoefer and Rome 1994). The 100-kDa major vault protein (MVP) makes up 70%–75% of the mass of the particle (Kedersha et al. 1991). The two minor vault proteins are the 193-kDa poly (ADP-ribose) polymerase and the 240-kDa telomerase-associated protein TEP1 (Kickhoefer et al. 1999a,b). However, the expression of MVP alone in bacteria or insect cells is sufficient to form vault-like particles (Stephen et al. 2001; Zheng et al. 2004).

Although many molecular features of vault particles have been characterized, the function of this large RNP remains enigmatic. The identification of lung-resistance related protein as the human MVP might imply a role of vaults in multi-drug resistance (Scheffer et al. 1995; for a review, see Mossink et al. 2003); however, direct involvement has been disputed (Van Zon et al. 2003a–c; Huffman and Corey 2005). Recent observations point to a role of vaults as scaffolds for signaling proteins (Yu et al. 2003; Kolli et al. 2004; Chung et al. 2005; Yi et al. 2005). Several studies suggest that vault protein may be involved in some form of intracellular transport (for a review, see Suprenant 2002), although the cargo has not yet been

identified. In the electromotor system of *Torpedo marmorata*, vaults are transported to the nerve terminal where they are allocated in close proximity to synaptic vesicles (Herrmann et al. 1996; Volknandt and Herrmann 1997). Anterograde and retrograde axonal transport of vaults has been analyzed in ligation experiments in which vaults accumulate on either side of the ligature (Li et al. 1999). Similarly, recombinant MVP assembled into vaults is targeted to neuritic tips of nerve growth factor (NGF)-treated phaeochromocytoma (PC12) cells (Herrmann et al. 1999). Extrapolation of data reported by Luby-Phelps and coworkers (1987) suggest that vaults are too large to diffuse freely in the cytosol. Therefore, vault interactions with cytoskeletal elements and molecular motors may be necessary for vault transport over longer distances. An association of vaults with microtubules both in vivo and in vitro has been reported (Hamill and Suprenant 1997; Eichenmüller et al. 2003). Furthermore, the colocalization of vaults and microtubules in PC12 and Chinese hamster ovary (CHO) cells has been described (Herrmann et al. 1999). An overlap of filamentous actin and vaults has been demonstrated in neuritic tips of PC12 cells and in ruffling edges of fibroblasts or CHO cells (Kedersha and Rome 1990; Herrmann et al. 1999).

To study the dynamics of vaults in living cells, we have created a fusion protein between the rat MVP and the green fluorescent protein (GFP) from the jellyfish *Aequoria victoria*. We demonstrate that this chimera assembles into vault-like particles and enables the study of the translocation of vault particles in living cells by fluorescence recovery after photobleaching (FRAP) and video microscopy. Our results indicate that individual vaults in the cytoplasm can be rapidly translocated.

Materials and methods

Cell culture and transfections

Cells were grown and maintained in Dulbecco's modified Eagle's medium (Gibco BRL, Bethesda, Md.) supplemented with either 10% fetal bovine serum (human astrogliomal U373 cells; a gift of F. Fahrenholz, University Mainz, Germany; COS7 cells, Irvine Scientific, Santa Ana, Calif.) or, in the case of the rat PC12 cell line (Herrmann et al. 1999), with 10% horse serum and 5% fetal calf serum (both Life Technologies, Paisley, Scotland, UK) containing penicillin and streptomycin (1% each; Sigma-Aldrich, Steinheim, Germany). Transfections of COS7 cells by 2 μg/ml supercoiled plasmid DNA were carried out either in the presence of 0.25 mg/ml DEAE-Dextran (Sigma, St. Louis, Mo.) in serum-free medium or in the presence of 3 μl FuGENE 6 (Boehringer-Mannheim) transfection reagent in complete medium. For DEAE-Dextran transfections, cells were incubated for 3–4 h at 37°C, followed by a 1-min treatment with 10% dimethylsulfoxide in buffer and a subsequent wash with serum-free medium. Complete medium was then added to the cells, which were harvested or viewed 48–72 h post-transfection. For FuGENE-6-mediated transfection, cells were incubated for 48 h in transfection medium and subsequently harvested or viewed. Phenol-red-free medium for viewing of viable cells was obtained from Gibco-BRL. PC12 and U373 cells were transiently transfected by electroporation by using 1–2 μg/ml GMVP construct. After plating, PC12 cells were treated with 10 ng/ml NGF (recombinant β-subunit; Sigma-Aldrich) for 48 h.

Vector construction

Vector construction was performed as described previously (Slesina et al. 2005). In brief, S65-T-GFP was amplified by the polymerase chain reaction from pGreen Lantern (Gibco-BRL) by using oligonucleotides containing a *Bsp*HI site; this allowed the subcloning of the entire GFP sequence in-frame into an *Nco*I site at the 5′ end of the cDNA encoding the rat MVP. This *Nco*I site contained the start codon of the MVP allowing for in-frame fusion of both full-length cDNAs. For transfection of PC12 and U373 cells, Green-Lantern-MVP was subcloned into the multiple cloning site of pcDNA3 vector containing a cytomegalovirus promoter (Invitrogen, Leek, Netherlands) and termed GMVP. The construct was confirmed by sequencing.

Fractionation of cells

COS7 cells transfected with GMVP were washed three times with ice-cold PBS and lysed at 2×10^7 cells/ml in buffer A (50 mM TRIS pH 7.4, 75 mM NaCl, 1.5 mM $MgCl_2$) containing 0.5% NP-40 on ice. Total cell lysates (T) were transferred to Eppendorf tubes, mixed thoroughly for 15 s, and centrifuged at $13{,}000g_{av}$ for 15 min at 4°C to generate a nuclear pellet (P1) and a supernatant fraction (S1). The supernatant fraction was centrifuged at $128{,}000g_{av}$ for 2 h to generate a soluble (S2) fraction, and a microsomal pellet (P2) fraction. All fractions were adjusted to equal volumes of lysis buffer. Further purification of the microsomal pellet was carried out by loading onto 10%–60% discontinuous sucrose gradients followed by centrifugation at $90{,}000g_{av}$ in a Sorvall AH650 rotor for 16 h at 4°C.

SDS-polyacrylamide gel electrophoresis and Western blotting

Aliquots of total cell homogenates or fractionated cells were run on 7.5%, 10%, 15%, or 5%–15% SDS-polyacryamide gels by published methods (Laemmli 1970). Proteins were visualized by electophoretic transfer to nitrocellulose (Amersham Lifescience) followed by immunoblotting with N2 polyclonal anti-vault antisera (Kedersha et al. 1990). Blots were blocked for a minimum of 30 min in TRIS-buffered saline (TBS) containing 0.5% Tween-20 and 5% nonfat dry milk and incubated with

primary antibody diluted in TBS containing 0.5% Tween-20 and 5% normal goat serum overnight at 4°C. Blots were washed (3×5 min each) with TBS containing 0.5% Tween-20, followed by incubation in secondary antibody coupled to horseradish peroxidase diluted in TBS containing 0.5% Tween-20 and 5% normal goat serum. Blots were developed by using enhanced chemiluminescent (ECL, Amersham) detection.

Immunocytochemistry

U373 cells were grown on poly-D-lysine-coated coverslips for 24–48 h and fixed in either ice-cold methanol for 7 min or phosphate-buffered saline (PBS: 137 mM NaCl, 3 mM KCl, 100 mM Na_2HPO_4, 18 mM KH_2PO_4, pH 7.3) solution containing 4% paraformaldehyde for 30 min followed by three washes in PBS containing 0.1% Triton X-100. Non-specific binding sites were blocked with 5% bovine serum albumin in PBS for 30 min. Subsequently, the primary antibodies were applied for 30 min. Polyclonal, monospecific anti-MVP104 (Herrmann et al. 1999), and/or monoclonal anti-β-tubulin (T-4026, Sigma, Deisenhofen, Germany) antibodies were used at a dilution of 1:100. To visualize filamentous actin, fluorescein isothiocyanate (FITC)-conjugated phalloidin was used at a dilution of 1:40. Cells were washed five times with PBS and incubated for 30 min with secondary antibodies (anti-mouse-FITC and/or anti-rabbit-Cy3 at a dilution of 1:100 or 1:500, respectively). To remove unbound antibody, cells were washed five times. Immunofluorescence was visualized by using a Zeiss Axiophot I equipped with an MCID 4 imaging analysis system (Imaging Research, St. Catharines, Canada) or a laser-assisted Leica TCS4D true confocal scanning microscope (CLSM). To visualize only colocalized fluorescence obtained in the two channels, immunosignals were multiplied with each other by using Adobe Photoshop 7.

Viewing of living cells

COS7 cells were viewed by using a Nikon Diaphot inverted microscope equipped for epifluorescent microscopy. Fluorescent filter sets for viewing GFP were obtained from Nikon (excitation 395 nm; emission 508 nm). S65-T mutated GFP was viewed by using standard FITC filter sets (excitation 488 nm; emission 511 nm). Cells were imaged with either a Photometrics KAF1400 cooled charge-coupled device (CCD) camera (Inovision, Princeton, N. J.) or a Zeiss LSM 410 Kr/Ar CLSM (Carl Zeiss, Thornwood, N.Y.) equipped with a 40× water objective. PC12 cells were viewed with a CLSM (Leitz DM IRB and TCS4D, Leica Lasertechnik, Heidelberg, Germany) equipped with a temperature control unit set at 37°C for living cells. The time interval between images was limited to 1.8 s. Video-enhanced microscopy of PC12 and U373 cells was performed by using an Axiovert 135 TV (Zeiss, Göttingen, Germany) and an intensified CCD camera (Extended ISIS, Photonic Science, PTI, Braunschweig, Germany) at 25 frames/s. The speed of vault particles was evaluated by measuring the traveled distance of individual particles between two subsequent images and dividing this value by the time interval (n=20).

FRAP experiments

In NGF-treated PC12 cells, FRAP experiments were performed by bleaching neurites (>25 μm length) and monitoring the reappearance of fluorescent particles at 1.8-s intervals. In order to minimize irritation of the cells and to reduce the robust fluorescence signal of GMVP in PC12 cells completely, bleaching was performed for 10–15 min at lower laser intensity.

Photobleaching of COS7 cells was carried out on a 12×9 μm^2 section of a cell at 100% laser power for 10 s. Recovery was monitored by scanning the entire cell at 3.5-s intervals at 40% laser power for 1 min.

Results

GMVP fusion protein is assembled into vault-like particles

The entire sequence of GFP was fused to the complete sequence of rat MVP at its amino terminus (see above). In vitro translation was used to confirm that fusion proteins of the correct size (~127 kDa) were produced (data not shown). To demonstrate that the addition of GFP to MVP did not interfere with the assembly of vault particles, the fractionation of endogenous MVP was compared with that of the GMVP fusion protein (Fig. 1a,b). After centrifugation of total cell homogenates (T) of non-transfected COS7 cells (Fig. 1a, lanes 1–5) the majority of MVP was retained in the postnuclear fraction (S1); however, some immunoreactivity could be seen in the nuclear pellet fraction (P1). MVP fractionated largely to the high speed pellet (P2 fraction) after recentrifugation of S1. No immunoreactivity was seen in the S2 fraction. The fractionation pattern of GMVP fusion protein (Fig. 1a, lanes 6–10) was identical to that of endogenous MVP, which was also present in the transfected cells.

To define whether the GMVP found in the P2 fraction was incorporated into a particle of the same density as a vault, the P2 fraction (P) from non-transfected and GMVP-transfected COS7 cells was applied to a 10%–60% step sucrose gradient, followed by Western blot analysis of the gradient fraction. Endogenous MVP fractionated to the 45% and 50% sucrose layers, characteristic of vaults (Fig. 1b, top). Both endogenous MVP (~100 kDa) and GMVP (~127 kDa) in transfected cells sedimented as MVP from non-transfected cells (Fig. 1b, bottom); however, GMVP-containing vaults were recovered in more fractions of the sucrose gradient (particularly the denser fractions) than genuine vaults, probably because of their extra mass.

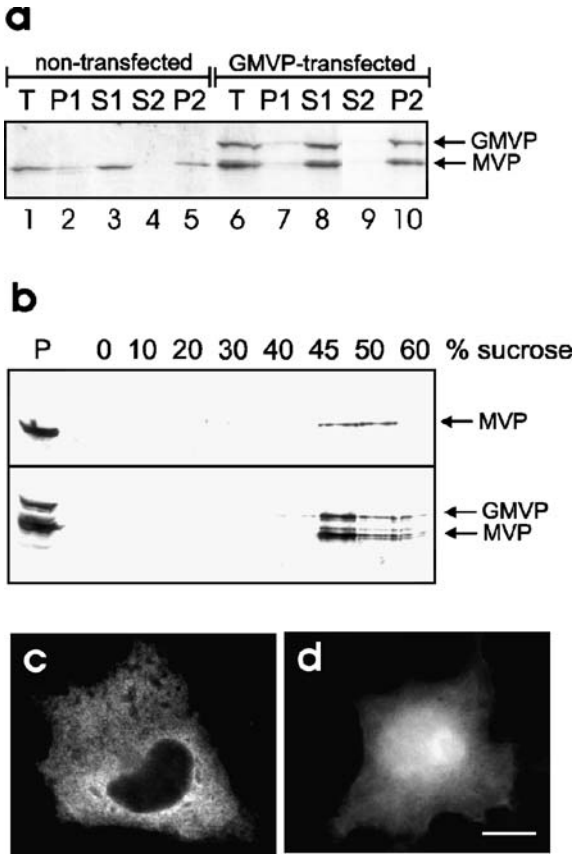

Fig. 1 GMVP fusion protein behaves like endogenous MVP. **a** Western blot of subcellular fractions derived from non-transfected (*lanes 1–5*) or GMVP-transfected (*lanes 6–10*) COS7 cells with the anti-MVP antibody (*T* total cell lysate, *P1* low-speed pellet, *S1* low-speed supernatant, *S2* high-speed supernatant, *P2* high-speed pellet, *arrows* positions of endogenous MVP and GMVP). Fractionation of GMVP is identical to that of endogenous MVP, indicating that this protein is able to interact with and form vault particles. Note that a significant, albeit small, amount of MVP and GMVP immunoreactivity also sediments within the nuclear fraction (*P1*). **b** Western blots of high speed pellet (*P* parent fraction P2) fractions from non-transfected (top), and GMVP-transfected (bottom) COS7 cells subjected to equilibrium centrifugation through 10–60% step sucrose gradients with MVP antibody (*arrows* positions of endogenous MVP and GMVP). GMVP fusion protein migrates at the same layers of the gradient as MVP from transfected and non-transfected cells, indicating incorporation into vaults. **c**, **d** Distribution of GMVP-fusion-protein (**c**) compared with GFP alone (**d**) in fixed COS7 cells. The GMVP-transfected cell shows punctuate cytoplasmic distribution, whereas the GFP-transfected cell shows a diffuse distribution of fluorescence in nucleus and cytoplasm. *Bar* 10 μm

In addition immunofluorescence revealed a particle allocation of expressed GMVP in transfected COS7 cells yielding thousands of fluorescent spots with a punctate and mainly cytoplasmic distribution characteristic of vaults (Fig. 1c). In contrast, the expression of GFP alone gave diffuse staining with a preferential nuclear localization (Fig. 1d). Thus, the chimera was considered suitable for the analysis of vault dynamics in living cells.

Bulk movement of vaults analyzed by FRAP in PC12 cells

FRAP allows the elimination of fluorescence in a defined area of a cell and the observation of the recovery of fluorescence within that area. We used the FRAP method for NGF-induced neuritic extensions of PC12 cells to monitor the speed and mobility of individual vault particles and bulk transport. Numerous translocations of fluorescent dots in a neurite of a living PC12 cell occurred between two subsequent confocal images (Fig. 2a,b). Although translocation of GMVP was easily depicted, evaluation of the movement of individual vault particles was almost impossible because of the high translocation velocity and the 1.8-s limitation in time resolution of the CLSM (see insets of Fig. 2a,b where vault translocation was frequent but could not be assigned to identifiable individual particles).

To evaluate the bulk movement of vaults, neurites of PC12 cells were photobleached intensively over a distance of approximately 25 μm, and the reappearance of fluorescence was monitored (Fig. 2c–f). Only a few fluorescent dots were localized in the tip of the neurite 90 s after photobleaching, whereas after 530 s, considerable numbers of fluorescent particles could be detected. Reappearance of fluorescence was mostly restricted to the neuritic tip and was rare in the neurite (Fig. 2d–f, bracket). Interestingly, no migration or diffusion front emerged from the unbleached cell body.

In transfected COS7 cells, a portion of the cell was rapidly photobleached (10 s) when viewed by a different CLSM at its highest laser power. Once the section of the cell was bleached, a series of images of the cell was taken to monitor recovery of vault fluorescence into the photobleached area. A panel of images from a typical experiment is shown in Fig. 3. Vault fluorescence recovered quickly and completely, filling in the bleached area within 14 s to 17.5 s (Fig. 3b–h), indicating that vault movement in the cytoplasm was rapid.

Video-enhanced microscopical analysis of vault movement

To gain further insight into vault motion, we performed video-enhanced microscopical analysis of GMVP motion in PC12 cells; this enabled us to reduce the time span between subsequent images to 0.04 s (25 frames/s). The translocation of GMVP chimeras appeared to be saltatory. Individual fluorescent spots moved rapidly over a short period of time and then came to a rest (Fig. 4, arrowheads). However, incidences of GMVP movement could be seen between subsequent images (Fig. 4a,b; insets illustrate movement in an anterograde direction during image acquisition, see arrow). The video-microscopical images (Fig. 4c,d) demonstrated that fast translocation of GMVP similarly took place in the astrogliomal cell line U373MG. For those cases in which motion could be assigned to individual particles or clusters of vaults, their velocity was

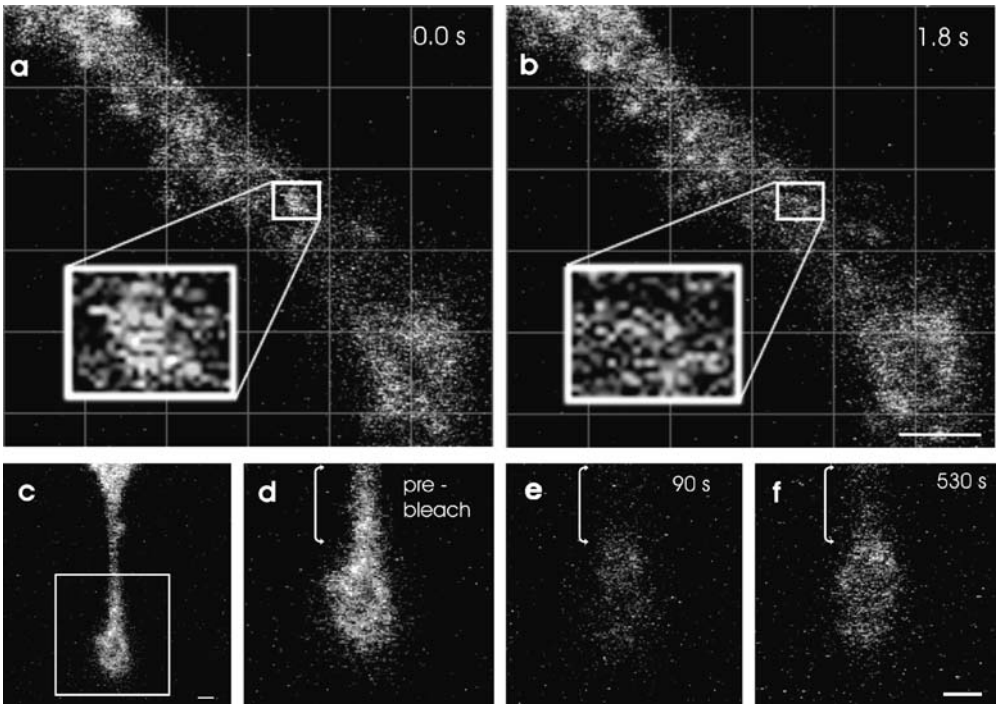

Fig. 2 Vault movements in cells as assessed by fluorescence recovery after photobleaching (FRAP). **a**, **b** Sequential confocal laser scanning images of GMVP fusion protein in the neurite of a differentiated PC12 cell. The neurite was partially photobleached to reduce fluorescence intensity (*insets* examples of frequent translocations of fluorescent material). **c**–**f** FRAP analysis of a neurite and neuritic tip of a PC12 cell (*bracket* neuritic stalk). **c** Overview (*inset* magnified area in **d**–**f**). **d** Neuritic tip before bleaching. **e** Same tip 90s after bleaching. **f** Same tip after a recovery period of 530 s. Note the reappearance of fluorescent material accumulating in the tip. *Bars* 2 μm

calculated to be 10±3 μm/s (n=20). However, measurement accuracy was hampered by the limited optical resolution, and we could not rule out that vaults moved in and out of the focal plane, instead of the actual vault particles being translocated.

Association of vaults with cytoskeletal elements

The evaluation of a specific interaction of vaults with cytoskeletal elements in the neurites of PC12 cells was hindered because of the dense packaging of microtubules. Therefore, we performed double-labeling experiments in U373MG cells in order to identify the cellular basis of vault movement. Vault particles were not colocalized with actin stress fibers (Fig. 5a–c). However, vaults accumulated in ruffling membranes at the growing ends of cells, similar to filamentous actin (Fig. 5a–c, arrows). In contrast, double-labeling of MVP and β-tubulin demonstrated the overlapping distribution of vaults with microtubules (Fig. 5d–f). Of note, the vaults were often arranged in a filamentous pattern along microtubules (Fig. 5d–f, arrow). Figure 5c,f demonstrates the merged fluorescence signals of MVP and the respective cytoskeletal element. The random alignment of vaults along a track became even more apparent at higher magnification (Fig. 5g, arrowheads).

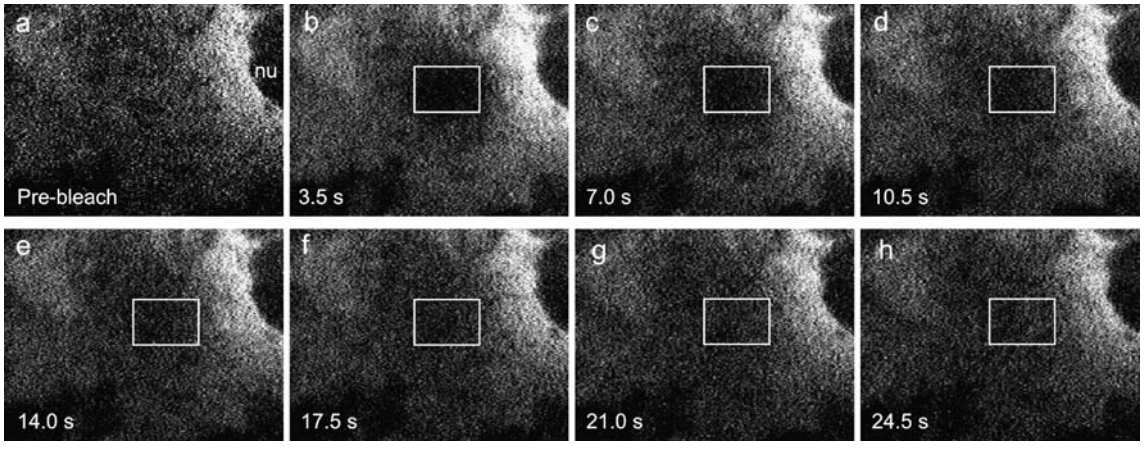

Fig. 3 Bulk movement of vaults as revealed by FRAP analysis. COS7 cell transfected with GLMVP construct shows punctate cytoplasmic distribution of fluorescence. Experiments were conducted on a Zeiss LSM 410 CLSM at 488 nm excitation. Photobleaching was carried out by scanning a 12×9 μm^2 section of a cell (*boxed*, **b**–**h**) at 100% laser power for 10 s. Recovery was monitored by capturing confocal images at 3.5-s intervals at 40% laser power for 1 m. **a** Cell prior to bleaching (*nu* nucleus). **b**–**h** Recovery of fluorescence into bleached area at 3.5-s intervals during 21 s postbleach

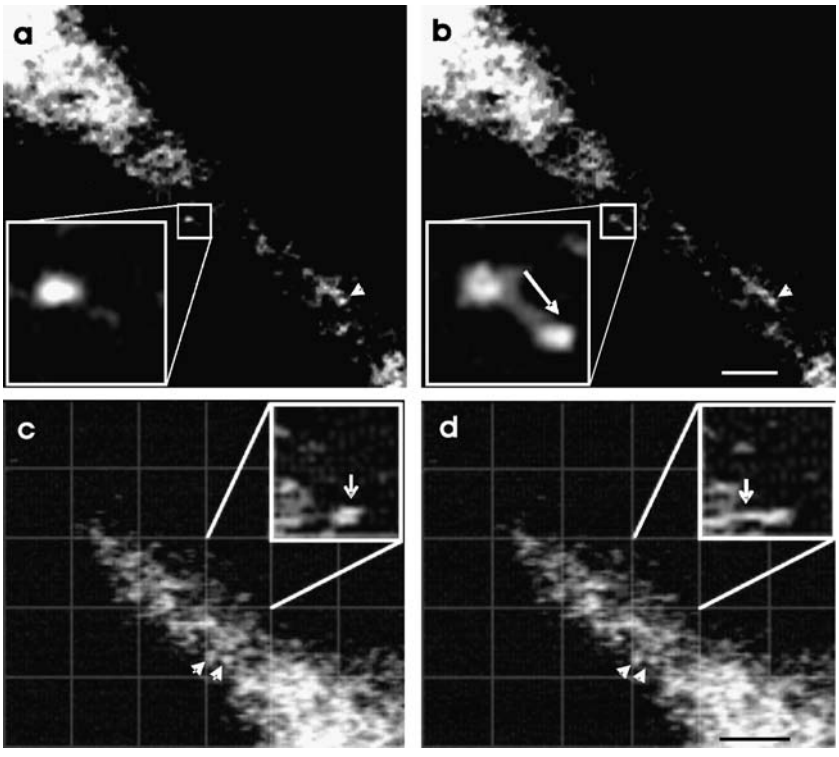

Fig. 4 Vaults move quickly. **a**–**d** Sequential video-microscopical images of GMVP fusion protein in cellular extensions of PC12 (**a**,**b**) and U373 (**c**,**d**) cells. The time interval between **a**/**b** or **c**/**d** is 0.04 s. *Arrows* in *insets* depict cases of rapid translocation of fluorescent material (*arrowheads* stationary fluorescent puncta). *Bars* 2 μm

Discussion

Dynamics of vault movement

Subcellular fractionation and immunofluorescence has demonstrated that our fusion construct behaves like endogenous MVP and assembles into vault-like particles. The GFP vault complex has been found in the cytosol of all cells investigated in this study in a similar punctate pattern as the endogenous vaults. Thus, the GMVP-fusion protein can be used to analyze vault dynamics in living cells. Video microscopy and fluorescence recovery after photobleaching (FRAP) have been performed on cell lines expressing GMVP fusion protein to analyze the movement of vaults. Analysis of MVP translocation by FRAP has allowed us to estimate the bulk transport of vaults and to distinguish

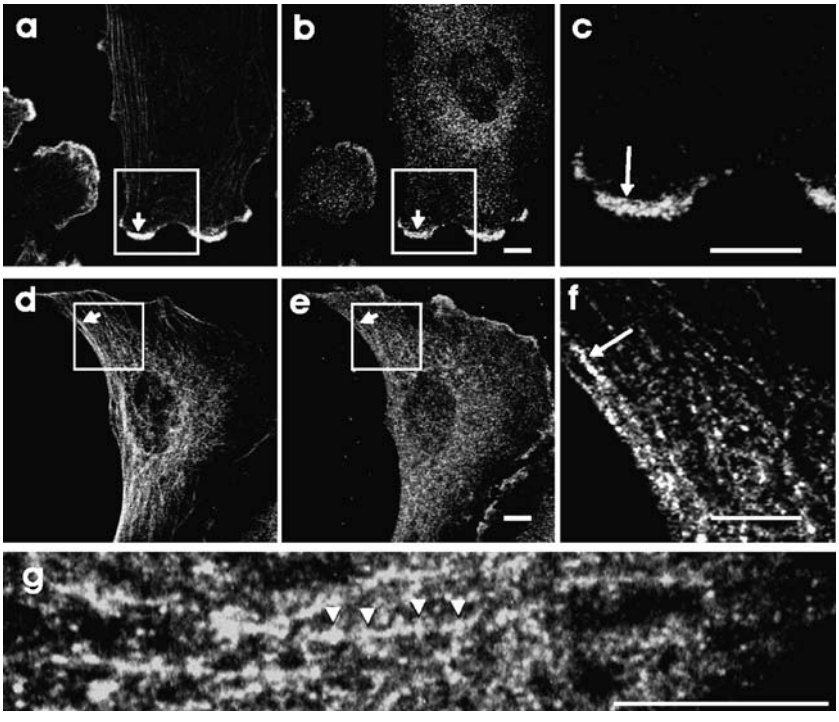

Fig. 5 Vaults colocalize with cytoskeletal elements in U373 cells. **a** CLSM image showing the distribution of filamentous actin detected by FITC-conjugated phalloidin in U373 cells. **b** CLSM demonstrating the distribution of MVP. **c** Magnification of **a**, **b** depicting only colocalized fluorescence. **d** CLSM image of the distribution of microtubules. **e** CLSM image showing the distribution of MVP. **f** Magnification of **d**, **e** depicting only colocalized fluorescence. *Arrows* indicate colocalization of MVP and the respective cytoskeletal element. **g** Immunocytochemistry with MVP antibody indicating that vaults are randomly aligned along tracks in the cytoplasm of U373 cells (*arrowheads*). *Bars* 10 μm

between fast transport and diffusion. Video microscopy has allowed us to monitor the movement of individual fluorescent spots. Earlier studies have demonstrated that vaults accumulate in cells in the ruffling edges of growth cones, neuritic tips, and presynaptic compartment, all of which would require transport over long distances (Kedersha and Rome 1990; Herrmann et al. 1999, 1996). Our FRAP analysis has demonstrated the migration and accumulation of vault particles into neuritic tips of PC12 cells. By applying a similar experimental approach, Van Zon and coworkers (2003a,b,c) have estimated the speed of vault particles to be approximately 2 μm/s, which is in the range of fast retrograde transport of vesicles (reviewed in Hammerschlag et al. 1994). They have observed no temperature dependence of vault motility and conclude that vaults move by diffusion. Their cell lines however express a large amount of MVP-GMP that does not become incorporated into vault particles and might interfere with measurements of intact vault motility. Based on the extrapolation of data, Luby-Phelps et al. (1987) consider intact vaults to be too large to diffuse freely in the cytosol. The lack of migration or a diffusion front observed in our study is indicative of fast active transport. This is consistent with our video-microscopical observations, although the accuracy of measurements of high velocity movements of individual vault particles is limited by the technical equipment and techniques employed. Our analysis of the velocity of vault movement over short distances in cellular extensions indicates that individual fluorescent spots are transported with a speed of about 10 μm/s, which is in the range of the well-documented fast anterograde axonal transport of synaptic vesicles along microtubules, viz., 400 mm/d in mammals (4.6 μm/s; reviewed in Vallee and Bloom 1991; Hammerschlag et al. 1994) and up to 5 μm/s at 21°C in the squid giant axon (Allen et al. 1982). A report by Kaether and coworkers (2000) who have also employed video-enhanced microscopy describes the maximal velocity of tagged synaptic vesicles as being 5 μm/s and of tubules containing tagged amyloid precursor protein as being 8–9 μm/s. The notion that vaults might be transported by a mechanism resembling fast axonal transport is further supported by ligature experiments in *Torpedo* electric nerves in which vaults accumulate on both sides of the crush point with an anterograde and retrograde component similar to that of synaptic vesicles (Li et al. 1999).

Association of vaults with microtubules

Both immunocytochemistry and cryo-immunoelectron microscopy have demonstrated an association of vault particles and microtubules in the cytoplasm of U373 cells. The colocalization of MVP and microtubules has also been shown for PC12 and CHO cells (Herrmann et al. 1999). Moreover, sea urchin vaults copurify with microtubules as described by Hamill and Suprenant (1997). In mammalian cells, vaults remain associated with tubulin oligomers even after nocodazol treatment (Eichenmüller et al. 2003). Using an in vitro microtubule pull-down assay and negative staining, Eichenmüller et al. (2003) have demonstrated that 5–6 vaults bind to 1-μm-long microtubules via their caps. A direct interaction of vaults and filamentous actin is less obvious. At the growing ends of the cell, MVP and filamentous actin are colocalized. The colocalization of actin fibers with MVP in the ruffling edges of rat fibroblasts has been reported, as has the colocalization of vaults with the ends of actin filaments at adhesion plaques (Kedersha and Rome 1990). Moreover, vaults and filamentous actin accumulate in the neuritic tips of differentiated PC12 cells similar to synaptic-like microvesicles (Herrmann et al. 1999). Whether the colocalization of vaults and actin fibers is attributable to the dense packaging of molecules in the cell periphery or to the direct interaction of actin filaments with vaults needs to be resolved. In neurons, the association of synaptic vesicles with microtubules changes to a synapsin-based interaction with actin filaments when the organelles enter the nerve terminal (Hosaka et al. 1999). Thus, in addition to microtubules, filamentous actin might be involved in vault transport.

Implications of vault transport

Our observations of the fast translocation of vaults support the hypothesis that vaults act as transport vehicles. The association of microtubules with vaults might explain how they reach their destinations in the cytoplasm and how they approach the nuclear pore complex (Chugani et al. 1993; Slesina et al. 2005).

Attempts to determine the role of MVP in multidrug resistance have led to the hypothesis that vaults function in the nuclear efflux of chemotherapeutic drugs (Kitazono et al. 1999, 2001; Dalton and Scheper 1999). Our observations support the postulated function of vaults as cytoplasmic shuttles, although their specific cargo and precise transport route have yet to be identified. Future studies are required to elucidate the mode of interaction between vaults and cytoskeletal elements and the motors involved in fast vault transport.

Acknowledgements The authors thank Dr. Valerie Kickhoefer and Prof. Herbert Zimmermann for reading the manuscript and making valuable suggestions.

References

Allen RD, Metuzals J, Tasaki I, Brady ST, Gilbert SP (1982) Fast axonal transport in squid giant axon. Science 218:1127–1129

Chugani DC, Rome LH, Kedersha NL (1993) Localization of vault particles to the nuclear pore complex. J Cell Sci 106:23–29

Chung J-H, Ginn-Pease ME, Eng C (2005) Phosphatase and tensin homologue deleted on chromosonme 10 (PTEN) has nuclear localization signal-like sequences for nuclear import mediated by major vault protein. Cancer Res 65:4108–4116

Dalton WS, Scheper RJ (1999) Lung resistance-related protein: determining its role in multidrug resistance. J Nat Canc Inst 91:1604–1605

Eichenmüller B, Kedersha N, Solovyeva E, Everly P, Lang J, Himes RH, Suprenant KA (2003) Vaults bind directly to microtubules via their caps and not their barrels. Cell Motil Cytoskeleton 56:225–236

Hamill DR, Suprenant KA (1997) Characterization of the sea urchin major vault protein: a possible role for vault ribonucleoprotein particles in nucleocytoplasmic transport. Dev Biol 190:117–128

Hammerschlag R, Cyr JL, Brady ST (1994) Axonal transport and the neuronal cytoskeleton. In: Siegel GJ, et al (eds) Basic neurochemistry: molecular, cellular, and medical aspects. Raven, New York, pp 545–571

Herrmann C, Volknandt W, Wittich B, Kellner R, Zimmermann H (1996) The major vault protein (MVP100) is contained in cholinergic nerve terminals of electric ray electric organ. J Biol Chem 271:13908–13915

Herrmann C, Golkaramnay E, Inman E, Rome LH, Volknandt W (1999) Recombinant major vault protein is targeted to neuritic tips of PC12 cells. J Cell Biol 144:1163–1172

Hosaka M, Hammer RE, Südhof TC (1999) A phospho-switch controls the dynamic association of synapsins with synaptic vesicles. Neuron 24:377–387

Huffman KE, Corey DR (2005) Major vault protein does not play a role in chemoresistance or drug localization in a non-small cell lung cancer cell line. Biochemistry 44:2253–2261

Kaether C, Skehel P, Dotti CG (2000) Axonal membrane proteins are transported in distinct carriers: a two-color video microscopy study in cultured hippocampal neurons. Mol Biol Cell 11:1213–1224

Kedersha NL, Rome LH (1986) Isolation and characterization of a novel ribonucleoprotein particle: large structures contain a single species of small RNA. J Cell Biol 103:699–709

Kedersha NL, Rome LH (1990) Vaults: large cytoplasmic RNPs that associate with cytoskeletal elements. Mol Biol Rep 14:121–122

Kedersha NL, Miquel MC, Bittner D, Rome LH (1990) Vaults. II Ribonucleoprotein structures are highly conserved among higher and lower eukaryotes. J Cell Biol 110:895–901

Kedersha NL, Heuser JE, Chugani DC, Rome LH (1991) Vaults. III Vault ribonucleoprotein particles open into flower-like structures with octagonal symmetry. J Cell Biol 112:225–235

Kickhoefer VA, Rome LH (1994) The sequence of a cDNA encoding the major vault protein from *Rattus norvegicus*. Gene 151:257–260

Kickhoefer VA, Searles RP, Kedersha NL, Garber ME, Johnson DL, Rome LH (1993) Vault RNP particles from rat and bullfrog contain a related small RNA that is transcribed by RNA polymerase III. J Biol Chem 268:7868–78173

Kickhoefer VA, Vasu SK, Rome LH (1996) Vaults are the answer, what is the question? Trends Cell Biol 6:174–178

Kickhoefer VA, Siva AC, Kedersha NL, Inman EM, Ruland C, Streuli M, Rome LH (1999a) The 193-kD vault protein, VPARP, is a novel poly(ADP-ribose) polymerase. J Cell Biol 146:917–928

Kickhoefer VA, Stephen AG, Harrington L, Robinson MO, Rome LH (1999b) Vaults and telomerase share a common subunit, TEP1. J Biol Chem 274:32712–32718

Kitazono M, Sumizawa T, Takebajashi Y, Chen ZS, Furokawa T, Nagayama S, Tani A, Takao S, Aikou T, Akiyama SI (1999) Multidrug resistance and the lung resistance-related protein in human colon carcinoma SW-620 cells. J Nat Canc Inst 91:1647–1653

Kitazono M, Okumura H, Ikeda R, Sumizawa T, Furukawa T, Nagayama S, Seto K, Aikou T, Akiyama SI (2001) Reversal of LRP-associated drug resistance in colon carcinoma SW-620 cells. Int J Cancer 91:126–131

Kolli S, Zito CI, Mossink MH, Wiemer EAC (2004) The major vault protein is a novel substrate for the tyrosine phosphatase SHP-2 and scaffold protein in epidermal growth factor signaling. J Biol Chem 279:29374–29385

Kong LB, Siva AC, Rome LH, Stewart PL (1999) Structure of the vault, a ubiquitious cellular component. Structure 7:371–379

Kong LB, Siva AC, Kickhoefer VA, Rome LH, Stewart PL (2000) RNA location and modeling of a WD40 repeat domain within the vault. RNA 6:1–11

Laemmli UK (1970) Cleavage of structural proteins during the assembly of the head of bacteriophage T4. Nature 227:680–685

Li JY, Volknandt W, Dahlström A, Herrmann C, Blasi J, Das B, Zimmermann H (1999) Axonal transport of ribonucleoprotein particles (vaults). Neuroscience 91:1055–1065

Luby-Phelps K, Castle PE, Taylor DL, Lanni F (1987) Hindered diffusion of inert tracer particles in the cytoplasm of mouse 3T3 cells. Proc Natl Acad Sci USA 84:4910–4913

Mossink MH, Van Zon A, Scheper RJ, Sonneveld P, Wiemer EAC (2003) Vaults: a ribonucleoprotein particle involved in drug resistance? Oncogene 22:7458–7467

Rome LH, Kedersha N, Chugani D (1991) Unlocking vaults: organelles in search of a function. Trends Cell Biol 1:47–50

Scheffer GL, Wijngaard PL, Flens MJ, Izquierdo MA, Slovak ML, Pinedo HM, Meijer CJ, Clevers HC, Scheper RJ (1995) The drug resistance-related protein LRP is the human major vault protein.Nat Med 1:578–582

Slesina M, Inman EM, Rome LH, Volknandt W (2005) Nuclear localization of the major vault protein in U373 cells. Cell Tissue Res 321:97–104

Stephen AG, Raval-Fernandez S, Huyn T, Torres M, Kickhoefer VA, Rome LH (2001) Assembly of vault-like particles in insect cells expressing only the major vault protein. J Biol Chem 276:23217–23220

Suprenant KA (2002) Vault ribonucleoprotein particles: sarcophagi, gondolas, or safety deposit boxes? Biochemistry 41: 14447–14454

Vallee RB, Bloom GS (1991) Mechanisms of fast and slow axonal transport. Annu Rev Neurosci 14:59–92

Van Zon A, Mossink MH, Scheper RJ, Sonneveld P, Wiemer EA (2003a) The vault complex. Cell Mol Life Sci 60:1828–1837

Van Zon A, Mossink MH, Schoester M, Houtsmuller AB, Scheffer GL, Scheper RJ, Sonneveld P, Wiemer EA (2003b) The formation of vault-tubes: a dynamic interaction between vaults and vault PARP. J Cell Sci 116:4391–4400

Van Zon A, Mossink MH, Schoester M, Scheper RJ, Sonneveld P, Wiemer EA (2003c) Efflux kinetics and intracellular distribution of daunorubicin are not affected by major vault protein/lung resitance-related protein (vault) expression. Cancer Res 64:4887–4892

Volknandt W, Herrmann C (1997) The major protein of a large ribonucleoprotein particle (VAULT) is localized in nerve terminals. In: Teelken AW, Korf J (eds) Neurochemistry: cellular, molecular, and clinical aspects. Plenum, London, pp 675–681

Yi C, Li S, Chen X, Wiemer EAC, Wang J, Wei N, Deng XW (2005) Major vault protein, in concert with constitutively photomorphogenic 1, negatively regulates c-jun-mediated activator protein 1 transcription in mammalian cells. Cancer Res 65:5835–5840

Yu Z, Fotouhi-Ardakani N, Wu L, Maoui M, Wang S, Banville D, Shen S-H (2003) PTEN associates with the vault particles in HeLa cells. J Biol Chem 277:40247–40252

Zheng C-L, Sumizawa T, Che X-F, Tsuyama S, Furukawa T, Haraguchi M, Gao H, Gotanda T, Jueng H-C, Murata F, Akiyama S-i (2004) Characterization of MVP and VPARP assembly into vaultribonucleoprotein complexes. Biochem Biophys Res Comm 325:100–107